# Cathodic Reduction of Bisulfite and Sulfur Dioxide in Aqueous Solutions on Copper Electrodes: An Electrochemical ESR Study

**Ian Streeter,[†] Andrew J. Wain,[†] James Davis,[§] and Richard G. Compton*,[†]**

*Physical and Theoretical Chemistry Laboratory, Oxford University, South Parks Road, Oxford OX1 3QZ, United Kingdom, and School of Biomedical and Natural Science, Nottingham Trent University, Nottingham NG11 8NS, United Kingdom*

*Received: April 8, 2005*

The electrochemical reduction of aqueous solutions of sulfite under acidic conditions on copper electrodes is reported, and a mechanism is proposed. Cyclic voltammetry at a copper disk suggests the operation of two reduction processes, the dominant process depending on solution pH. At very low pH (0−2), sulfur dioxide is reduced in a two-electron, two-proton reaction, but at higher pH (2−5), bisulfite is the electroactive species, being reduced by a single electron to ultimately yield the $SO_2^{\bullet -}$ radical anion. Simultaneous electrochemical electron spin resonance (ESR) measurements using a tubular flow cell support this proposal, and suggest that the radical anion is in equilibrium with dithionite, which is found to decay at low pH. Digisim modeling of the system is shown to be consistent with this mechanism over the experimental pH range.

## Introduction

The electrochemical reduction of aqueous solutions of sulfur dioxide has been the subject of numerous investigations dating back to the 1930s, and a wide variety of electrode materials have been studied, including mercury,[1−6] gold,[7,8] platinum,[9] bismuth,[10] copper,[11,12] iron phthalocyanine modified graphite,[13] and the iron alloy Uranus B6.[14] The origin of such attention stems mainly from the use of this process in the electrogeneration of sodium dithionite (sodium hydrosulfite), an important and very widely used industrial reducing agent,[15] but interest in sulfur dioxide electrochemistry also lies in electroanalysis. For example, sulfite, which is in equilibrium with sulfur dioxide in aqueous solution, is commonly used as a preservative in the food industry,[16] but exposure at high levels has been known to have toxic effects, such as respiratory distress in asthmatic patients, hypotension, and gastrointestinal problems;[17] therefore, its determination (electrochemical or spectroscopic) is of much significance.[6,11,12,18] For the electroanalytical approaches to be reliable and successful, it is clearly essential that the mechanistic aspects of the electrochemical processes are fully understood, and that has been the focus of many of the previous studies.

It has been recognized for some years that the sulfite anion ($SO_3^{2-}$), when dissolved in aqueous solution, is in equilibrium with both bisulfite ($HSO_3^-$) and sulfur dioxide, their relative concentrations depending on the solution pH, and numerous protonation and hydration equilibria have been postulated,[19,20] which can be simplified as the following:

$$SO_3^{2-} + H^+ \rightleftharpoons HSO_3^- \quad (1)$$

$$HSO_3^- + H^+ \rightleftharpoons SO_2 + H_2O \quad (2)$$

Equilibrium constants for the above have been reported in the literature, and despite some variation, the values $K_1 = 1.5 \times 10^7$ mol$^{-1}$ dm$^3$ and $K_2 = 71.9$ mol$^{-1}$ dm$^3$ at 298 K for reactions 1 and 2, respectively, appear to be generally accepted.[19−22] It should be noted that $K_2$ has been defined here such that it incorporates the activity of $H_2O$ ($K_2 = [SO_2]/[HSO_3^-][H^+]$), and so, rather than being dimensionless, the reported value has units of mol$^{-1}$ dm$^3$. Using the above acidity constants, it is simple to calculate the relative equilibrium concentrations of the three sulfur-containing species as a function of pH,[20] and the result can be seen in Figure 1, in which the quantity plotted on the vertical axis is the amount of each species as a mole fraction of the total sulfur in solution. It is clear from this that above about pH 8, sulfite is the dominant aqueous species, bisulfite dominates in the range $3 < pH < 7$, whereas below approximately pH 1, sulfur dioxide is the major sulfur-containing species in solution. An equilibrium must also exist between dissolved sulfur dioxide and that in the gaseous phase; however, throughout this work we have assumed the effects of this are negligible on the time scale of the experiments undertaken, and as such, this will not be considered further. It will become clear that the speciation described above is of utmost importance when considering the electrochemical behavior of such solutions, and will therefore be referred to repeatedly throughout this work.

Several mechanisms have been posed for the polarographic reduction (mercury electrodes) of aqueous sulfur dioxide, in which multiple cathodic waves have often been observed.[5] Gosman[1] proposed that, under highly acidic conditions, the major electron-transfer pathway was the single-electron reduction of hydrated sulfur dioxide ($SO_2{\cdot}OH_2$, or $H_2SO_3$) to form dithionous acid ($H_2S_2O_4$), whereas Kolthoff and Miller[2] suggested that the two-electron, two-proton reduction of sulfur dioxide to yield sulfoxylic acid ($H_2SO_2$) was a more likely electrode process. They also hypothesized that the electroactive species in mildly acid media was bisulfite ($HSO_3^-$), as suggested by the speciation curves in Figure 1, and that it is reduced by a single electron, generating the $HSO_2^{\bullet}$ radical. The notion that the identity of the electroactive species changes with pH was also later suggested by Reynolds and Yuan,[5] who observed up to four polarographic waves. Contrary to these earlier conclu-

* To whom all correspondence should be addressed. Email: richard.compton@chemistry.oxford.ac.uk. Tel.: +44 (0) 1865 275 413. Fax.: +44 (0) 1865 275 410.

[†] Oxford University.

[§] Nottingham Trent University.

10.1021/jp058119n CCC: $30.25 
Published on Web 09/08/2005

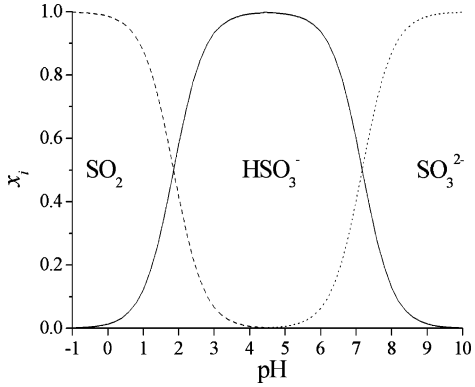


**Figure 1.** Equilibrium concentrations of sulfur-containing species in aqueous solution, expressed as a mole fraction of the total sulfur, $x_i$, for i = $SO_2$, $HSO_3^-$, or $SO_3^{2-}$, as a function of pH.

sions, Tolmachev and Scherson[10] conjectured that sulfur dioxide is the sole electroactive agent, even under relatively weakly acidic conditions (pH 3−6), and that the voltammetric current attributed to its one-electron reduction is limited by the rate of sulfur dioxide formation from bisulfite (reaction 2), in a CE-type mechanism. However, since the above interpretations were based on the voltammetry at a bismuth rotating-disk electrode, it is difficult to draw a direct comparison with those results obtained using a dropping mercury electrode, since differences may arise as a result of specific interactions of the substrate with the electrode material. Nevertheless, the conflicting observations suggest that there may still be some doubt as to the fundamental mechanistic aspects of this electrochemical system.

In this paper, the voltammetric reduction of aqueous solutions of sulfite is interrogated on copper electrodes, and a mechanism is proposed in which a two-electron-transfer mechanism operates at very low pH (<2), but a single-electron process takes place under less acidic conditions (up to pH 5), wherein the sulfur dioxide radical anion is generated. We report the detection of this paramagnetic species in situ, using the technique of simultaneous electrochemical ESR and employing a hydrodynamic tubular flow cell, and show that signal intensity measurements are consistent with the reaction mechanism proposed. The mechanism is further supported by Digisim modeling of the quiescent voltammetry over the pH range studied.

## Theory

**1. Hydrodynamic Flow in a Tube.** The theory describing simultaneous electrochemical ESR measurements for paramagnetic species electrogenerated using a tubular flow cell has been reported previously,[23] and has been recently developed with more rigor.[24,25] It is well established that the convection−diffusion equation for mass transport in a cell of tubular geometry is given by[26]

$$\frac{\partial c}{\partial t} = D\left(\frac{\partial^2 c}{\partial x^2} + \frac{\partial^2 c}{\partial r^2} + \frac{1}{r}\frac{\partial c}{\partial r}\right) - v_x\frac{\partial c}{\partial x} \qquad \text{(I)}$$

where $D$ and $c$ are the diffusion coefficient and concentration of the electroactive species, respectively, $r$ and $x$ are the radial and axial coordinates, and $v_x$ is the flow velocity in the axial direction. When the solution flow is sufficiently fast enough that effects of axial diffusion are masked by convection, the $\partial^2 c/\partial x^2$ term can be neglected, and similarly, if we assume that the diffusion layer of the electrode is thin, it is possible to ignore the radial $1/r$ term. The convection term can be evaluated by considering a laminar flow profile, shown schematically in Figure 2, and can also be simplified under conditions of a thin diffusion layer, which allows the flow parabola to be linearized (the Lévêque approximation), reducing equation I to

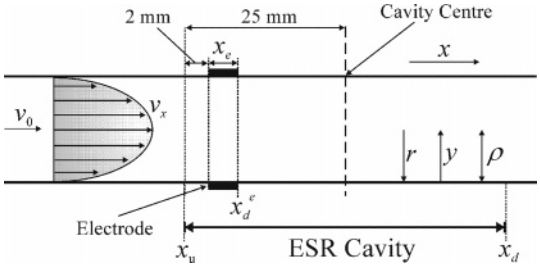


**Figure 2.** Schematic of the tubular flow cell and parabolic flow profile, including the relative position of the electrode within the ESR cavity.

$$\frac{\partial c}{\partial t} = D\frac{\partial^2 c}{\partial y^2} - \frac{2v_0 y}{\rho}\frac{\partial c}{\partial x} \qquad \text{(II)}$$

where $v_0$ is the axial velocity at the tube center, $\rho$ is the tube radius, and $y$ is the radial coordinate relative to the tube wall. Analytical solution of this simplified mass-transport equation at steady state yields the Levich equation for the limiting current ($i_{lim}$) at a tubular electrode:[25,27]

$$i_{lim} = 5.24 \times 10^5 n[A]_{bulk} D^{2/3} x_e^{2/3} V_f^{1/3} \qquad \text{(III)}$$

where $n$ is the number of electrons transferred, $[A]_{bulk}$ is the bulk concentration of electroactive species, $x_e$ is the length of the electrode (nominally 3 mm in this work), and $V_f$ is the volume flow rate (found by integrating the axial flow velocity over the tube radius).

**2. ESR Signal Intensity.** ESR signal intensity ($S$) gives a measure of the total number of radicals in the sensitive region of the resonant cavity. Thus, by integrating the concentration profile throughout the volume of the cell that is downstream of the electrode (see Figure 2), and by convoluting this with the $\sin^2 x$ sensitivity profile in the ESR cavity,[23] we deduce the following:

$$S = S_0\int_{x_d^e}^{x_d} \sin^2\left(\frac{x - x_u}{l}\pi\right)\int_0^{\rho} 2\pi r c(r,x)\, dr\, dx \qquad \text{(IV)}$$

where $S_0$ is the signal measured for 1 mol of ESR active species at the cavity center, $x_u$ and $x_d$ are the coordinates of the upstream and downstream edge of the cavity, respectively, $x_d^e$ is the coordinate of the downstream edge of the electrode, $l$ is the length of the cavity, and $c$ is the concentration of the electrogenerated ESR active species.

It has been shown that substitution of the concentration profile obtained from the solution of the mass-transport equation into the above integral leads to the following general relationship:[23]

$$\frac{S}{i_{lim}} \propto \frac{1}{V_f^{2/3}} \qquad \text{(V)}$$

Since the above considerations have only involved a simple electron transfer to generate a paramagnetic species, with no follow-up homogeneous chemistry, equation V holds only for radicals that are stable on the experimental time scale, and deviation from this relationship is often indicative of radical decay. However, since this has been derived under the assumption of the Lévêque approximation, it is not necessarily valid at all flow rates, but this is not a constraint since it is possible

to simulate the concentration profile fully using numerical methods.[24,25] Furthermore, previous studies would suggest that equation V holds for the flow rates employed in this work.

## Experimental Section

**1. Chemical reagents.** Sodium sulfite ($Na_2SO_3$), sodium dithionite ($Na_2S_2O_4$), and TEMPO (2,2,6,6-tetramethylpiperidine-*N*-oxyl) were purchased from Aldrich. Britton-Robinson buffer solutions were made using 0.04 M acetic, phosphoric (both BDH), and boric (Sigma) acids, and were adjusted to the required pH using NaOH (Aldrich). Sulfuric acid solutions were prepared from concentrated $H_2SO_4$ (BDH). Water used to make the electrolyte solutions, with a resistivity of not less than 18 MΩ cm, was taken from a Synergy water purification system (Millipore). All reagents used were of the highest commercially available grade and were used without further purification.

**2. Preparation of Solutions.** Before solutions of sulfite were prepared, all electrolyte solutions were degassed with oxygen-free nitrogen (BOC Gases, Guildford, Surrey, U.K.) for at least 15 min. Adding sodium sulfite to aqueous acid generates $SO_2$, which is one of the electroactive species being studied, and so no further bubbling was applied once the solutions were prepared so as not to drive the dissolved gas out of solution. However, during the voltammetric and ESR experiments, a gentle stream of nitrogen was allowed to pass over the surface of the solution in order to prevent oxygen from reaching the electrolyte, without significantly perturbing the $SO_2$ equilibrium.

**3. Apparatus.** Ex situ voltammetry was carried out on a 1.0-mm diameter copper macro-disk working electrode, with a platinum coil counter electrode (Goodfellow, Cambridge, U.K.) and a saturated calomel reference electrode (SCE, Radiometer, Copenhagen, Denmark). Potential control was achieved using a computer-controlled PGSTAT30 potentiostat (Autolab, Eco Chemie, Utrecht, The Netherlands).

In situ electrochemical ESR experiments were carried out using a copper tube flow cell of internal diameter 1 mm, having the same design as that characterized previously.[24] A platinum gauze counter electrode was positioned downstream of the 3-mm long copper working electrode, and an SCE reference was placed upstream. As a result of the highly resistive nature of the cell design, it was necessary to attach a 0.1 $\mu$F capacitor between the reference and counter electrodes in order to ensure electronic stability under steady state potentiostat control. Fluid motion was maintained using a gravity flow system, employing glass capillaries to achieve slower flow rates. The volume flow rates achieved were in the range $0.21 \times 10^{-3}$ to $96 \times 10^{-3}$ cm$^3$ s$^{-1}$.

ESR spectra were obtained using a JEOL JES-FA100 X-band spectrometer with a cylindrical ($TE_{011}$) cavity resonator.[28] The cell was positioned in this cavity such that the distance between the upstream edge of the electrode and the end of the sensitive region of the cavity (see Figure 2) measured 2 mm. Cavity tuning was achieved using the JEOL spectrometer software (A-SYSTEM v.1.100, FA-MANAGER v.1.01). To account for variations in cavity Q, we measured signal intensities relative to a standard marker consisting of MgO dispersed with $Mn^{2+}$, inserted into the cavity at the time of measurement. In all of the experiments, a microwave power of 1 mW was used, and regular tests were carried out to check that increasing the microwave power increased the ESR signal. Doing so ensured that the system was not power saturated such that the ESR signal intensity gave a direct measure of the number of electrogenerated spins in the cavity.[28] All experiments were conducted at 20 ± 2 °C.

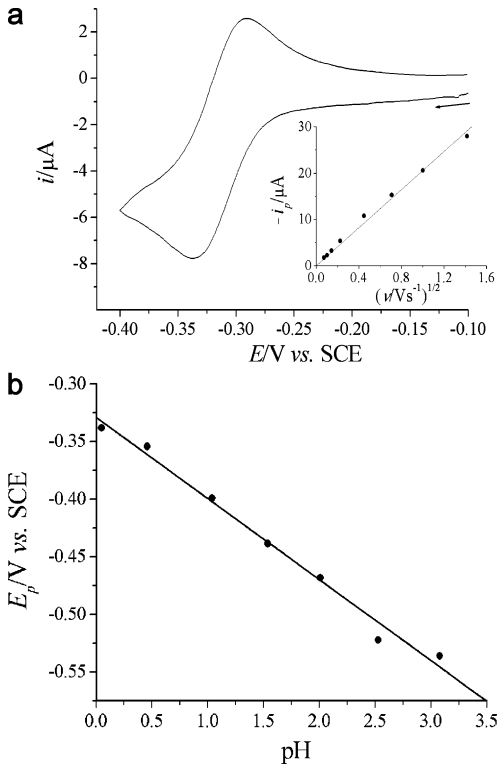


**Figure 3.** (a) Cyclic voltammetry at 100 mV s$^{-1}$ on a 1-mm diameter copper disk electrode of a 1 mM solution of $Na_2SO_3$ in 1 M aqueous $H_2SO_4$ (pH 0). Inset: Variation of reduction peak current with square root of scan rate. (b) Reduction peak potential as a function of pH.

## Results and Discussion

**1. Copper Disk Voltammetry.** Preliminary voltammetric investigations into the reduction of aqueous sulfite on platinum, gold, and copper electrode substrates revealed that the latter gave by far the cleanest electrochemistry, and as such, all further investigations were carried out on this material. This rather unexpected observation is possibly a result of the different roles of adsorption of the electroactive sulfur-containing species on the various electrode surfaces. The electrochemical reduction of an aqueous solution of 1 mM sodium sulfite was first investigated on a 1-mm diameter copper disk electrode in strong acid (1 M $H_2SO_4$, pH 0), in which an electrochemically and chemically reversible redox couple was observed with an $E_{mid}$ at −0.32 V vs SCE and a peak-to-peak separation close to 60 mV, as shown in Figure 3a for a scan rate of 100 mV s$^{-1}$. Peak currents were found to be proportional to the square root of the scan rate in the range 5−2000 mV s$^{-1}$, indicative of a diffusion-controlled process[29] (see inset, Figure 3a), with a slope of $2.08 \times 10^{-5}$ A V$^{-1/2}$ s$^{1/2}$ that was used to calculate a value for the diffusion coefficient of the electroactive species according to the Randles-Ševčík equation for an electrochemically reversible couple.[29] The calculation was carried out on the basis of both one- and two-electron processes, and yielded diffusion coefficients of $9.7 \times 10^{-5}$ and $1.2 \times 10^{-5}$ cm$^2$ s$^{-1}$, respectively. On the basis of the speciation of aqueous sulfur species depicted in Figure 1, at pH 0 and 293 K, $SO_2$ is the dominant species in solution, and since reported values for its diffusion coefficient are close to $1.6 \times 10^{-5}$ cm$^2$ s$^{-1}$,[2,5,30] it was concluded that the latter of the above two calculated values was more reasonable and thus the reduction wave likely corresponds to a two-electron reduction per molecule.

Variable pH experiments in the range 0−3 ($H_2SO_4$, unbuffered) revealed that the reduction peak potential shifted in the negative direction by approximately 59 mV per pH unit (see

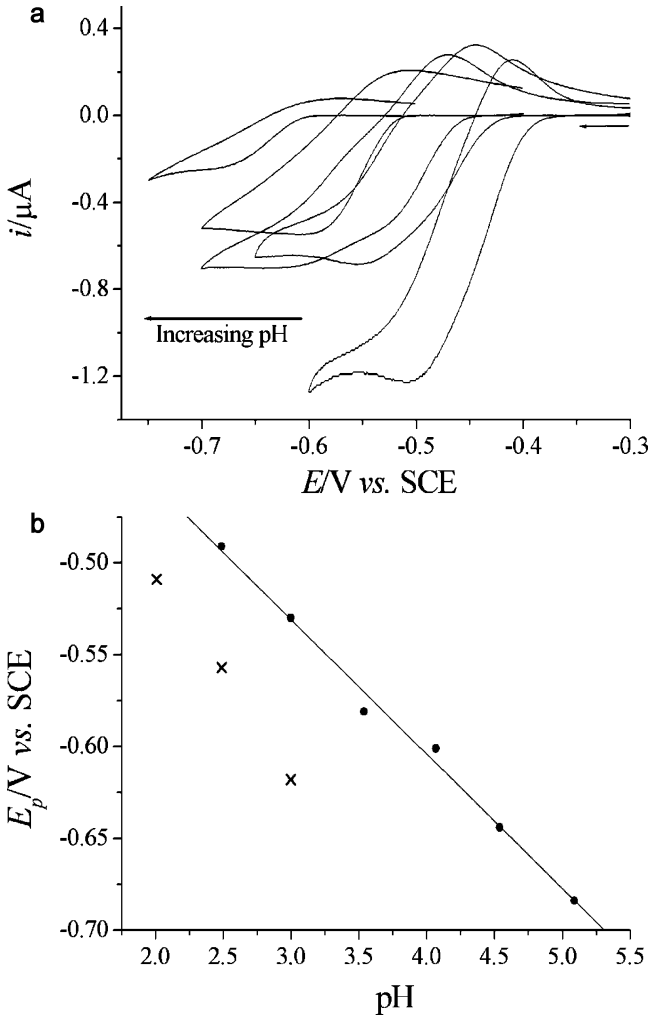


**Figure 4.** (a) Cyclic voltammetry at 5 mV $s^{-1}$ of a 2 mM solution of $Na_2SO_3$ in a 0.12 M Britton-Robinson aqueous buffer solution at pH 2.0, 2.5, 3.0, 4.1, and 5.1. (b) Reduction peak potentials at 5 mV $s^{-1}$ as a function of pH (crosses represent additional peak potentials in the cases where more than one wave was present).

Figure 3b), suggesting an *n*-electron, *n*-proton process.[29] The above observations suggest that under very acidic conditions, the cathodic wave corresponds to the two-electron, two-proton reduction of aqueous sulfur dioxide:

$$SO_2 + 2e^- + 2H^+ \rightleftharpoons H_2SO_2 \qquad (3)$$

The above interpretation is consistent with that suggested by Kolthoff and Miller,[2] who studied the polarographic reduction of $SO_2$ dissolved in aqueous $HNO_3$.

Next, the voltammetric behavior of aqueous sulfite solutions was investigated in the pH range 1.8−5.1, using 0.12 M Britton-Robinson buffer as supporting electrolyte. Figure 4a depicts a selection of cyclic voltammograms for 2 mM sulfite at a scan rate of 5 mV $s^{-1}$, in which it is evident that the redox wave becomes broadened and less reversible with increasing pH. Moreover, there is evidence of double peaks, or shoulders, on the reduction waves in the region of pH 3−4 that are not apparent at any other pH, which might suggest the introduction of an additional process that becomes more dominant at higher pH (interestingly, these split waves were not so apparent at higher scan rates). The magnitudes of the voltammetric currents were found to diminish with increasing pH such that above pH 5.1, no reduction wave was visible, the process likely being

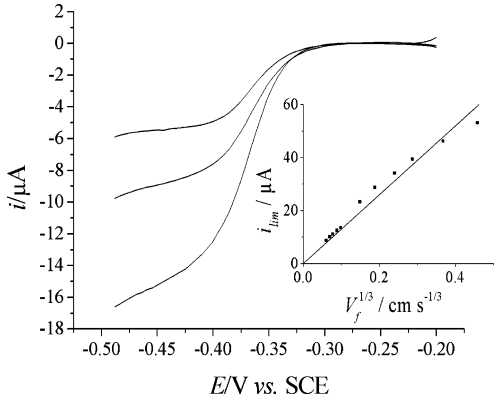


**Figure 5.** Hydrodynamic voltammetry of 2 mM aqueous $Na_2SO_3$ in pH 1.8 Brtitton-Robinson buffer, using a copper tube flow cell at volume flow rates of 3, 14, and 96 × $10^{-3}$ $cm^3$ $s^{-1}$. Inset: Plot of limiting current against the cube root of the volume flow rate.

obscured by the onset of solvent breakdown. With the speciation suggested in Figure 1 in mind, we interpreted the additional peaks as contributions from the reduction of $HSO_3^-$, which appears to be present above pH 1, and is the dominant species in solution above about pH 3. The reduction peak potentials for this scan rate are plotted as a function of pH in Figure 4b. In the cases where a double reduction wave was visible, two points were plotted, but these values should be treated with caution, since the broadened waves resulted in a significant degree of uncertainty in the peak position. Despite this, it is clear that the points in Figure 4b follow one of two lines, the set of six points with the more positive $E_p$ having a slope close to 59 mV per pH unit, which strongly suggests the participation of two reduction processes. It is reasonable to assume that one of these processes (i.e. the one dominating at lower pH) is the same as that described above for the voltammetry in strong sulfuric acid. Given the drop in cathodic current with increasing pH, we therefore postulate that the second process corresponds to the single-electron, single-proton reduction of $HSO_3^-$ to yield the sulfur dioxide radical anion and water:

$$HSO_3^- + e^- + H^+ \rightarrow SO_2^{\bullet -} + H_2O \qquad (4)$$

We propose that above pH 3 this reaction is dominant, and the voltammetry appears to become less reversible, which is likely a result of follow-up chemistry of the electrogenerated radical anion, which is known to dimerize, generating dithionite:[31−33]

$$2SO_2^{\bullet -} \rightleftharpoons S_2O_4^{2-} \qquad (5)$$

It is apparent from Figure 4a that with increasing pH, the reduction peak current drops to below half of that at very low pH, which might appear to be inconsistent with the proposed mechanism, but reaction 4 *requires* the protonation step (as indicated by the Nernstian behavior), and so the reduction process becomes limited by the proton concentration as pH increases.

Since reaction 4 involves the generation of paramagnetic species, electrochemical ESR was next used to probe the reaction mechanism further.

**2. Electrochemical ESR.** The electrochemical ESR was undertaken using a tubular flow cell for which the theory describing the mass transport has been well developed, and is outlined in the Theory section. Figure 5 shows typical linear sweep voltammetry depicting the reduction of a 2 mM solution of sulfite in pH 1.8 Britton-Robinson buffer using the flow cell,

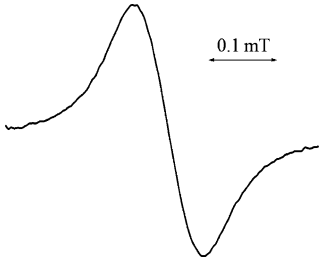


**Figure 6.** Typical ESR spectrum observed upon electrolysis of 5 mM solutions of $Na_2SO_3$ in the pH range 1.8−5.0, employing a modulation width of 0.1 mT.

including a plot of limiting current as a function of volume flow rate (inset).

Electrolysis of the 2 mM sulfite solution at pH 1.8 using the flow cell within the ESR cavity led to the observation of a single-line spectrum of width close to 0.1 mT, although the signal intensity was relatively weak compared to those from previous investigations of stable radicals electrogenerated in appreciable concentrations.[24] Further ESR experiments were thus undertaken using sulfite concentrations of 5 mM. Similar spectra were observed in the pH range 1.8−5.0, a typical spectrum being shown in Figure 6. The lack of any hyperfine structure makes identification of the paramagnetic species responsible for the spectrum difficult, but the single line is consistent with literature reports of the $SO_2^{\bullet-}$ radical anion, shown previously to be present in aqueous solutions of dithionite according to reaction 5.[34,35] Furthermore, these authors report a *g*-value of 2.0055 ± 0.0002 for this radical anion, which is in good agreement with the approximate *g*-value of 2.0053 ± 0.0001 recorded from the spectra observed in our work, which supports the notion that the sulfur dioxide radical anion is the species being detected by ESR in this case.

With the above interpretation in mind, we carried out ESR signal intensity measurements using the tubular cell at various flow rates in the pH range 1.8−5.0, and the current-normalized signal intensities are plotted in Figure 7 as a function of flow rate. It is evident that for a given flow rate, $S/i_{lim}$ increases with increasing pH, which is consistent with the interpretations inferred from the copper disk voltammetry. Under highly acidic conditions, reaction 3 is dominant, in which no paramagnetic species are generated, which, combined with the high limiting currents as a result of it being a two-electron process, leads to a low $S/i_{lim}$. As the solution pH is increased and the contribution from reaction 4 becomes significant, $SO_2^{\bullet-}$ radical anions are generated in more appreciable concentrations, and the limiting currents are correspondingly lower, leading to an increase in $S/i_{lim}$. Note that the absolute signal intensity, *S*, and the ratio $S/i_{lim}$ are dependent on the bisulfite concentration; this is shown below to be a result of the dimerization equilibrium (reaction 5).

So far reactions 3 and 4 have rationalized the experimental observations both voltammetrically and in the ESR measurements, but in order to evaluate the signal intensity data more quantitatively, we need to consider the fate of the $SO_2^{\bullet-}$ radical anions, and the chemistry observed *downstream* of the electrode in the tubular cell. The dimerization of $SO_2^{\bullet-}$ radical anions (reaction 5) has been studied in aqueous solution by a number of authors, and the equilibrium is known to lie heavily to the right-hand side in favor of dithionite, with reported equilibrium constants being on the order of $10^9$ mol$^{-1}$ dm$^3$.[31−33] It has further been suggested in the literature that the $SO_2^{\bullet-}$ radical anion−dithionite equilibrium is very quickly established, with dimerization rate constants close to being diffusion-controlled.[31,36] It

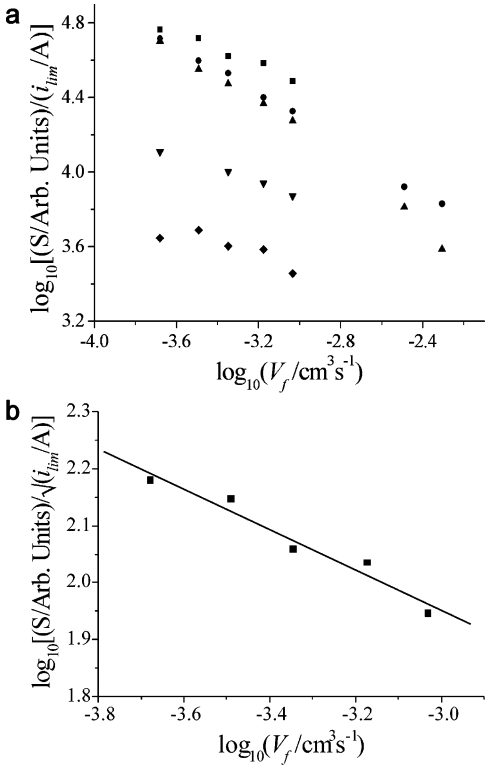


**Figure 7.** (a) Current-normalized ESR signal intensity ($S/i_{lim}$) as a function of volume flow rate for 5 mM aqueous solutions of $Na_2SO_3$ at pH 5.0 (■), pH 4.1 (●), pH 3.1 (▲), pH 2.5 (▼), and pH 1.8 (◆). (b) Plot of $\log(S/\sqrt{i_{lim}})$ against log of volume flow rate for the pH 5.0 data.

is therefore reasonable to propose that once the flowing electrolyte solution has reached the sensitive region of the ESR cavity, the homogeneous chemistry has taken place such that the ESR signal intensity is a measure of the local *equilibrium* concentration of $SO_2^{\bullet-}$ radical anions, which likely accounts for the weak signals observed. Since dithionite is by far the dominant component of the solution at this point, it is possible to consider the overall electrode reaction above pH 4 as follows:

$$2SO_2 + 2e^- \rightarrow S_2O_4^{2-} \qquad (6)$$

Since the electrogenerated dithionite is a stable species being detected downstream, we would expect the local concentration of $S_2O_4^{2-}$ to scale with $i_{lim}/V_f^{2/3}$, according to eq V. The local concentration of the equilibrated $SO_2^{\bullet-}$ is given by

$$K_{eq} = \frac{[S_2O_4^{2-}]}{[SO_2^{\bullet-}]^2} \qquad (VI)$$

where $K_{eq} \gg 1$. We therefore expect the ESR signal intensity of the paramagnetic $SO_2^{\bullet-}$ measured downstream of the electrode to be proportional to $\sqrt{i_{lim}/V_f^{2/3}}$. Hence, a plot of $\log(S/\sqrt{i_{lim}})$ against log of volume flow rate should have a slope of −1/3. Figure 7b shows such a plot for the data obtained at pH 5.0 (the highest pH studied, and therefore the least likely to be complicated by the parallel processes taking place at lower pH), which has a slope of −0.36, suggesting that the proposed mechanism is valid, and that a stable equilibrium (reaction 5) is being observed.

It appears from Figure 7a that the plots at pH 5.0, 4.1, and 3.1 are approximately linear, whereas at pH 2.5 and 1.8, there is some degree of curvature, suggesting that the radical anion

**TABLE 1: ESR Signal Intensity Measurements[a] of 0.1 M Solutions of Dithionite in Aqueous Britton-Robinson Buffer**

| pH | *S*/*M* | spin concentration (M) | $K_{eq}$ ($M^{-1}$)[b] |
|---|---|---|---|
| 9.3 | 3.4 | $7.9 \times 10^{-6}$ | $1.6 \times 10^{9}$ |
| 6.8 | 3.1 | $7.2 \times 10^{-6}$ | $1.9 \times 10^{9}$ |
| 4.6 | 3.7 | $8.5 \times 10^{-6}$ | $1.4 \times 10^{9}$ |
| 2.5 | 1.8 | $4.2 \times 10^{-6}$ | $5.6 \times 10^{9}$ |

[a] Quoted relative to marker signal (*S*/*M*). [b] Calculated equilibrium constants for reaction 5.

**SCHEME 1: Proposed Mechanism for the Electrochemical Reduction of Aqueous Solutions of Sulfite**

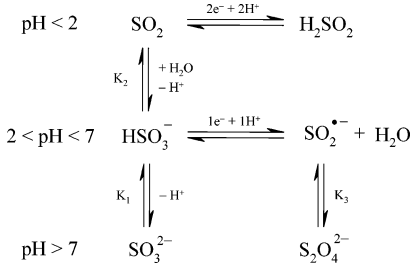


equilibrium is unstable under more acidic conditions (i.e., the signal intensity is less than predicted due to homogeneous decay of the paramagnetic species, which is more pronounced at slower flow rates). To investigate this, and to verify the dithionite equilibrium constant under the experimental conditions employed throughout the electrochemical ESR, the ESR spectra of solutions of 0.1 M sodium dithionite were recorded at various pH (Britton-Robinson buffer), and in each case the equilibrium concentration of radical anions was estimated by comparing the signal intensity to that of a solution of 1 mM aqueous TEMPO (2,2,6,6-tetramethylpiperidine-*N*-oxyl, a commonly employed stable radical standard) solution under the same conditions. The results are given in Table 1. The equilibrium constants deduced are in good agreement with those reported in the literature and, except for the value at pH 2.5, appear to be relatively pH independent, which is again consistent with documented findings.[31−33] This is what one would expect, given that no protons are involved in the equilibrium, but numerous studies have also revealed that dithionite itself is unstable under acidic conditions (pH <4) which rationalizes the higher equilibrium constant determined for the pH 2.5 solution.[36−39] In fact, the ESR signal intensity measured at this pH was found to drop over the course of the experiments, albeit relatively slowly, which reflects the reduction of the radical anion concentration as the dithionite decomposes. To determine an approximate time scale for the decay, we recorded transient ESR signal-intensity scans at pH 2.6 under less-concentrated conditions (10 mM dithionite), which revealed a total loss of signal after about 800 s. Although a more thorough analysis of the transients was not possible due to the complexity of the decomposition reaction, it is reasonable to conclude that the decay of dithionite is not fast enough to affect the quiescent voltammetry, but may have an effect on the electrochemical ESR signal measurements, given the slow flow rates employed. These observations therefore serve to rationalize the deviation from linearity in Figure 7a for pH 1.8 and 2.5.

Thus far the experimental observations made are consistent with reactions 3, 4, and 5, and so it was envisaged that further evidence supporting this proposed mechanism could be acquired from digital simulation of the copper disk voltammetry using Digisim.

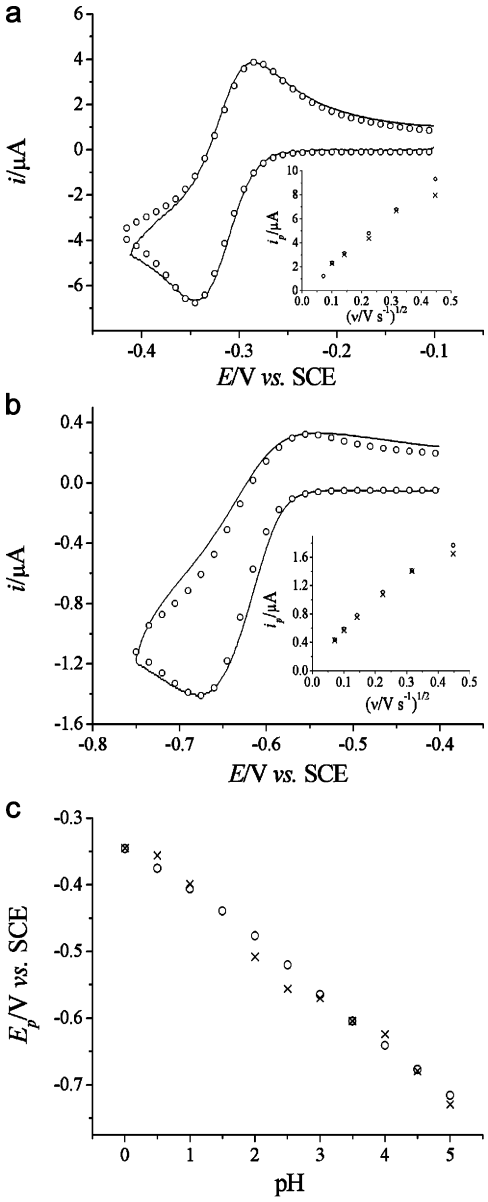


**Figure 8.** Digisim modeling (see text). Experimental (—) and simulated (○) voltammetry (100 mV $s^{-1}$) at (a) pH 0 and (b) 4.5. Insets: experimental (×) and simulated (○) reduction peak currents plotted against the square root of the scan rate. (c) Experimental (×) and simulated (○) peak potentials as a function of pH (at 100 mV $s^{-1}$).

**3. Digisim Modeling.** For clarity, the mechanism proposed is summarized in Scheme 1, which forms the basis of the model used in Digisim.[40] Given the speciation described in Figure 1, it is fair to assume that, in the pH range considered in this work, reaction 1 has no significant effect on the voltammetry, and so modeling was carried out considering reaction 2 only, using reactions 3 and 4 as heterogeneous steps. Since Digisim is incapable of simulating simultaneous electron−proton transfers, it was necessary to include protonation steps as separate, homogeneous reactions with diffusion-controlled rate constants in order to mimic Nernstian behavior. In addition to the literature value for $K_2$ (7.9 $mol^{-1}$ $dm^3$)[19,20] and $K_3$ determined above ($10^9$ $mol^{-1}$ $dm^3$), the following parameters were used to fit the voltammetry: reaction 3, $E_0 = -0.41$ V (vs SCE), $\alpha = 0.5$, $k_0 = 15$ cm $s^{-1}$; reaction 4, $E_0 = -0.52$ V (vs SCE), $\alpha = 0.5$, $k_0 = 1000$ cm $s^{-1}$ (it should be emphasized here that the heterogeneous rate constants used are fictitious in the sense that they were selected to optimize the fit, and so their absolute

values do not necessarily bear physical significance). Literature diffusion coefficients[8,30] of $1.6 \times 10^{-5}$ and $0.7 \times 10^{-5}$ $cm^2$ $s^{-1}$ were employed for sulfur dioxide and bisulfite, and these values were also used for all other uncharged and charged species, respectively.

Using the above parameters, it was possible to achieve good fits of the copper disk voltammetry across the pH range studied. Simulated voltammograms at 100 mV $s^{-1}$ are shown in panels a and b of Figure 8 for the two extremes of pH considered (pH 0 and 4.5, respectively), and show good agreement with the experimental voltammetry under these conditions. Shown inset are the variations of reduction peak currents with the square root of the scan rate, in which simulated and experimental results are again in good agreement. Further support of the mechanism can be seen in Figure 8c, which depicts the simulated and experimental reduction peak potentials, measured at 100 mV $s^{-1}$, plotted as a function of pH.

## Conclusions

Voltammetric and electrochemical ESR measurements have been shown to support the mechanism depicted in Scheme 1 for the reduction of aqueous solutions of sulfite on copper electrodes, in the pH range 0−5. Under highly acidic conditions ($0 < pH < 2$), the electroactive species is sulfur dioxide, which undergoes a two-electron, two-proton reduction, whereas in mildly acidic media ($2 < pH < 5$), bisulfite is reduced in a one-electron, one-proton step. The product of the latter reaction, after loss of water, is the $SO_2^{\bullet -}$ radical anion, which has been detected using a tubular electrochemical ESR cell. The ESR signal intensity was found to increase with pH, reflecting the transition from the two-electron process to the one-electron process, and the variation of signal strength with flow rate suggests that the paramagnetic species is stable during the ESR cell transit time under mildly acidic conditions, but less so at very low pH. It is proposed that the ESR signal measures the concentration of the radical anion in equilibrium with its dimer, dithionite, which is found to decay on the ESR experimental time scales employed. Digisim modeling of this relatively complex system provided further support of the mechanism proposed in the pH range 0−5.

**Acknowledgment.** We thank the EPSRC and JEOL for funding.

## References and Notes

(1) Gosman. *Collect. Czech. Chem. Commun.* **1937**, *2*, 185.
(2) Kolthoff, I. M.; Miller, C. S. *J. Am. Chem. Soc.* **1941**, *63*, 2818.
(3) Cermák, V. *Collect. Czech. Chem. Commun.* **1958**, *23*, 1871.
(4) Jacobsen, E.; Sawyer, D. T. *J. Electroanal. Chem.* **1967**, *15*, 181.
(5) Reynolds, W. L.; Yuan, Y. *Polyhedron* **1986**, *5*, 1467.
(6) Almeida, P. J.; Rodrigues, J. A.; Guido, L. F.; Santos, J. R.; Barros, A. A.; Fogg, A. G. *Electroanalysis* **2003**, *15*, 587.
(7) Quijada, C.; Huerta, F. J.; Morallón, E.; Vázquez, J. L.; Berlouis, L. E. A. *Electrochim. Acta* **2000**, *45*, 1847.
(8) Tolmachev, Y. V.; Wang, Z.; Hu, Y.; Bae, I. T.; Scherson, D. A. *Anal. Chem.* **1998**, *70*, 1149.
(9) Quijada, C.; Vázquez, J. L.; Perez, J. M.; Aldaz, A. *J. Electroanal. Chem.* **1994**, *372*, 243.
(10) Tolmachev, Y. V.; Scherson, D. A. *J. Phys. Chem. A* **1999**, *103*, 1572.
(11) Isaac, A.; Livingstone, C.; Wain, A. J.; Compton, R. G.; Davis, J. *Trends Anal. Chem.* **2005**, submitted for publication.
(12) Isaac, A.; Wain, A. J.; Compton, R. G.; Livingstone, C.; Davis, J. *Analyst* **2005**, Submitted for publication.
(13) Yu, C. S.; Choi, H.; Kim, S. *Chem. Lett.* **2002**, 648.
(14) Benayada, A.; Bessiere, J. *Electrochim. Acta* **1985**, *30*, 593.
(15) Scott, L. L.; Ding, Y.; Stalder, S. M.; Kohl, P. A.; Winnick, J.; Bottomley, L. A. *J. Electrochem. Soc.* **1998**, *145*, 4052.
(16) Chichester, D. F.; Tanner, F. W. In *Handbook of Food Additives*; Furia, T. E., Ed.; CRC Press: Cleveland, OH, 1972; p 115.
(17) Schwartz, H. J. *J. Allergy Clin. Immunol.* **1983**, *71*, 487.
(18) Smith, V. J. *Anal. Chem.* **1987**, *59*, 2256.
(19) Guthrie, J. P. *Can. J. Chem.* **1979**, *57*, 454.
(20) Siddiqi, M. A.; Krissmann, J.; Peters-Gerth, P.; Luckas, M.; Lucas, K. *J. Chem. Thermodyn.* **1996**, *28*, 685.
(21) Huss, A.; Eckert, C. A. *J. Phys. Chem.* **1977**, *81*, 2268.
(22) Johnstone, H. F.; Leppla, P. W. *J. Am. Chem. Soc.* **1934**, *56*, 2233.
(23) Albery, J. W.; Chadwick, A. T.; Coles, B. A.; Hampson, N. A. *J. Electroanal. Chem.* **1977**, *75*, 229.
(24) Wain, A. J.; Thompson, M.; Klymenko, O. V.; Compton, R. G. *Phys. Chem. Chem. Phys.* **2004**, *6*, 4018.
(25) Thompson, M.; Klymenko, O. V.; Compton, R. G. *J. Electroanal. Chem.* **2005**, *575*, 329.
(26) Levich, V. G. *Physicochemical Hydrodynamics*; Prentice Hall: New York, 1962.
(27) Blaedel, W. J.; Olson, C. L.; Sharma, L. R. *Anal. Chem.* **1963**, *35*, 2100.
(28) Weil, J. A.; Bolton, J. R.; Wertz, J. E. *Electron Paramagnetic Resonance, Elementary Theory and Practical Applications*; John Wiley and Sons: New York, 1994.
(29) Bard, A. J.; Faulkner, L. R. *Electrochemical Methods, Fundamentals and Applications*, 2nd ed.; John Wiley and Sons: New York, 2001.
(30) Samec, Z.; Weber, J. *Electrochim. Acta* **1975**, *20*, 413.
(31) Lynn, S.; Rinker, R. G.; Corcoran, W. H. *J. Phys. Chem.* **1964**, *68*, 2363.
(32) Neta, P.; Huie, R. E.; Ross, A. B. *J. Phys. Chem. Ref. Data* **1988**, *17*, 1031.
(33) Chien, J. C. W.; Dickinson, L. C. *J. Biol. Chem.* **1978**, *253*, 6965.
(34) Reuveni, A.; Luz, Z.; Silver, B. L. *J. Chem. Phys.* **1970**, *53*, 4619.
(35) Ozawa, T.; Setaka, M.; Kwan, T. *Bull. Chem. Soc. Jpn.* **1971**, *44*, 3473.
(36) Cermák, V.; Smutek, M. *Collect. Czech. Chem. Commun.* **1975**, *40*, 3241.
(37) Holman, D. A.; Bennett, D. W. *J. Phys. Chem.* **1994**, *98*, 13300.
(38) Burlamacchi, L.; Guarini, G.; Tiezzi, E. *J. Chem. Soc., Faraday Trans.* **1969**, *65*, 496.
(39) Kovács, K. M.; Rábai, G. *Chem. Commun.* **2002**, 790.
(40) Rudolph, M.; Reddy, D. P.; Feldberg, F. W. *Anal. Chem.* **1994**, *66*, 589A.